Modern Valence Bond Description of the Electronic Mechanisms of S_N2 Identity Reactions

Joshua J. Blavins,[†] David L. Cooper,*[,‡] and Peter B. Karadakov*[,†]

Department of Chemistry, University of York, Heslington, York YO10 5DD, U.K., and Department of Chemistry, University of Liverpool, Liverpool L69 7ZD, U.K.

Received: November 4, 2003; In Final Form: November 30, 2003

Series of ab initio modern valence bond calculations, based on spin-coupled (SC) theory, along the MP2(fc)/6-31G(d,p) minimum-energy paths, are used to examine the electronic rearrangements that take place during the gas-phase S_N2 identity reactions of Cl^- with RCl, where R is methyl, ethyl, or *tert*-butyl. The corresponding reaction of F^- with CH_3F is also considered. The SC descriptions of the two $CH_3X + X^-$ reactions (X = F or Cl) are found to be qualitatively similar, but there is a significantly larger extent of bond formation at the transition state for the fluorine case, and the electronic rearrangements also start much sooner. Comparing $CH_3Cl + Cl^-$ and $CH_3CH_2Cl + Cl^-$, the SC calculations suggest that the electronic structure reorganization is largely unaffected by the presence of the additional methyl group. The description of the transition state for the corresponding gas-phase S_N2 identity reaction of $(CH_3)_3CCl$ is found to be radically different: it is held together by predominantly ionic interactions and most closely resembles a carbocation "clamped" between two chloride ions.

Introduction

A recent high-level theoretical study of gas-phase S_N2 identity reactions

$$X^- + CH_3X \rightarrow CH_3X + X^-$$

has been presented by Lee and co-workers,[1] for X = H, F, Cl, and Br. Those authors, who reference much of the extensive literature on such systems, used methods up to QCISD(T) with a large 6-311++G(3df,2p) basis set and found good agreement with the available experimental data on geometries, energy barriers, and complexation energies. These S_N2 identity reactions reactions proceed via the formation of a very short-lived C_{3v}-symmetry $X^-...CH_3X$ ion−dipole complex which exhibits rather poor energy transfer between vibrations of the long weak C...X bond and the internal vibrational modes of CH_3X. The reactant-like complex is converted into an equivalent one, based on products, via a single kinetic step involving a trigonal bipyramidal (D_{3h}) transition state, with barrier heights for X = F and Cl on the order of 10−15 kcal/mol. The $X^-...CH_3X$ complexation energies for these two systems are also of this magnitude, but the complexes are significantly destabilized by various solvents and they may be completely absent in some situations, such as in aqueous solution. Definitive calculations of the energetics of the stationary points for various gas-phase $CH_3X + F^-$ S_N2 reactions have been reported by Gonzales and co-workers,[2] who provide further references to the extensive literature in this area.

Somewhat less theoretical work has been reported for the corresponding reactions involving larger alkyl groups. Of particular relevance to the present study are the MP2/6-31G(d) calculations of Jensen[3] for the gas-phase S_N2 identity reactions of Cl^- with RCl. The steric bulk of R certainly influences the height of the central barrier, but for small alkyl groups, the basic mechanism remains similar to the one described above for methyl. As anticipated, significant differences were observed in the case of *tert*-butyl. A subsequent study by Mohamed and Jensen[4] reexamined the same $Cl^- + RCl$ reactions in the presence of small numbers of molecules of water or other solvents, with the intention of studying the reduced steric effects in solution. They found increases in the S_N2 barrier heights but only relatively small changes in the transition state geometries, except in the case of the *tert*-butyl system. An interesting feature of all of these various calculations, whether in the gas phase or with "microsolvation", is that rotations about C−C bonds can lead to small differences between the lengths of the making and breaking C−Cl bonds at the transition state. The extent of this slight asymmetry, which implies two symmetry-equivalent reaction paths, varies with the level of calculation (e.g., MP2 vs B3LYP) and with the degree of microsolvation.

In the present work we use ab initio modern valence bond theory, in its spin-coupled form, to monitor the electronic rearrangements taking place during gas-phase S_N2 identity reactions of RCl with Cl^-, where R is methyl, ethyl, or *tert*-butyl. The corresponding reaction of CH_3F with F^- is also studied. We examine the bonding in the reactant-like ion−dipole complexes and the central transition states and then follow the reaction pathway. Comparison of the two $CH_3X + X^-$ reactions (X = F or Cl) yields insights into the differences due to the stronger nucleophile, F^-. Similarly, comparison of the various chlorine systems provides information relating to the consequences of additional methyl groups at the active site.

Computational Procedure

The geometries of the transition states and of the reactant-like ion−dipole complexes were optimized using restricted Hartree−Fock [RHF/6-31G(d,p)], density functional theory [B3LYP/6-31G(d,p)], and second-order Møller−Plesset perturbation theory [MP2(fc)/6-31G(d,p)]. The optimized transition state (TS) geometries were confirmed as first-order saddle points on the corresponding energy hypersurfaces through diagonalization of the analytical Hessians calculated at these geometries,

* To whom correspondence should be addressed.
[†] University of York.
[‡] University of Liverpool.

10.1021/jp037348b CCC: $27.50
Published on Web 01/08/2004

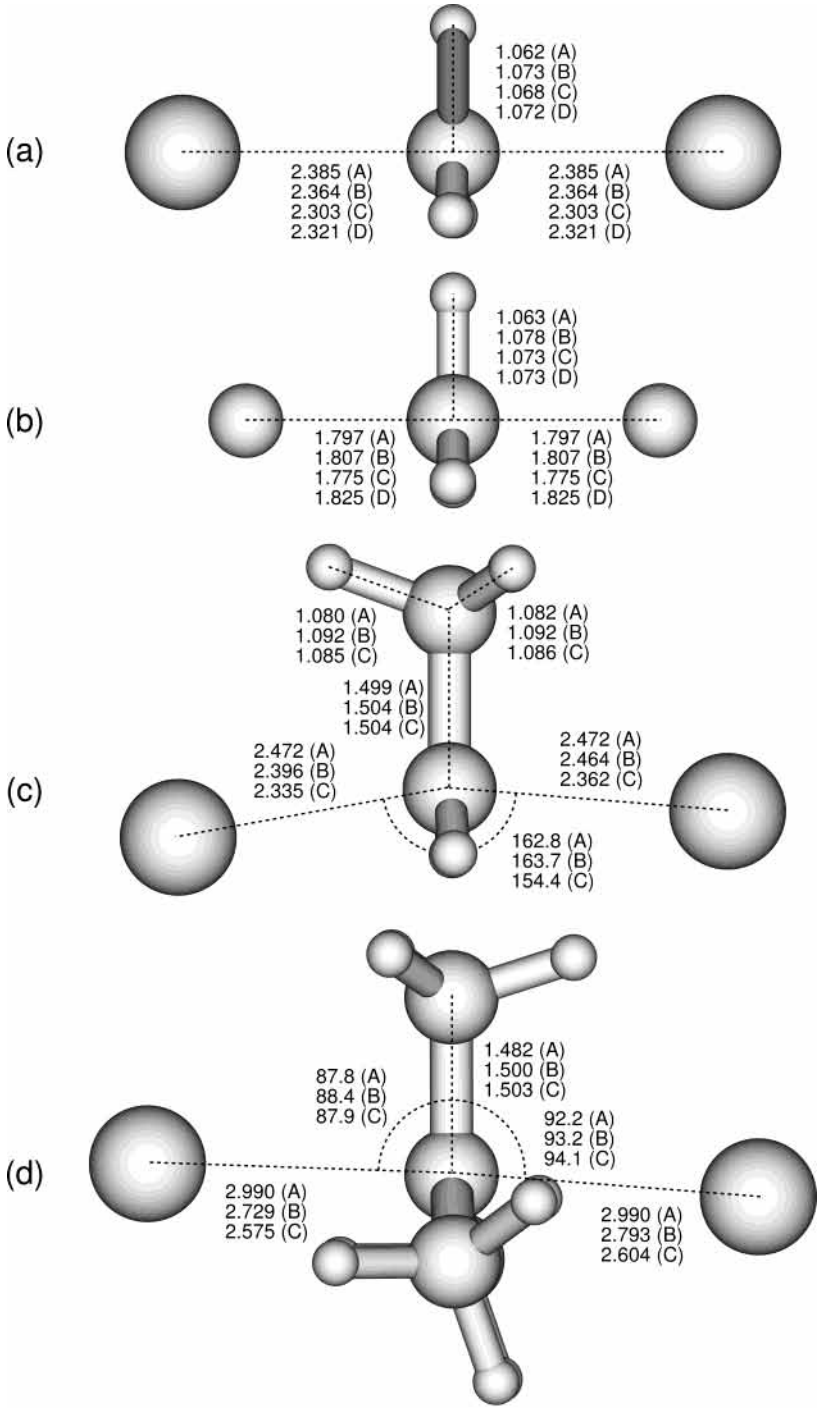

Figure 1. Key features of geometries for transition states in the gas-phase S_N2 identity reactions: (a) $CH_3Cl + Cl^-$; (b) $CH_3F + F^-$; (c) $CH_3CH_2Cl + Cl^-$; (d) $C(CH_3)_3Cl + Cl^-$. Calculations are labeled: (A) RHF/6-31G(d,p); (B) B3LYP/6-31G(d,p); (C) MP2/6-31G(d,p); (D) QCISD(T)/6-311++G(3df,2p),[1] with bond lengths in angstroms and angles in degrees.

with analogous checks that the ion−dipole complexes represent minima on the respective potential energy surfaces. The intrinsic reaction coordinate or IRC was then calculated at the MP2(fc)/6-31G(d,p) level of theory using standard procedures[5] implemented within Gaussian 98,[6] starting at the TS geometry and moving in steps of about 0.1 amu$^{1/2}$ bohr, until local minima were reached in the directions of the reactants and products. All geometry optimizations were carried out under the tight convergence criteria, with the default criteria for the IRC calculations. In the case of $(CH_3)_3CCl + Cl^-$, only the transition state was considered.

The generally accepted notion is that these reactions involve four active electrons, two from the forming σ bond and two from the breaking σ bond. For each system, we use modern valence bond, spin-coupled (SC) wave functions based on a single spatial configuration consisting of $N = 4$ fully optimized, nonorthogonal, one-electron "active" orbitals ψ_μ, together with a set of n fully optimized, orthogonal, doubly occupied "inactive" orbitals ϕ_i. In general, the SC wave function takes the form[7]

$$\Psi = \hat{A}[(\prod_{i=1}^{n}\phi_i\alpha\phi_i\beta)(\prod_{\mu=1}^{N}\psi_\mu)\Theta_{SM}^{N}] \qquad (1)$$

where Θ_{SM}^{N} is the active-space spin function (for N electrons

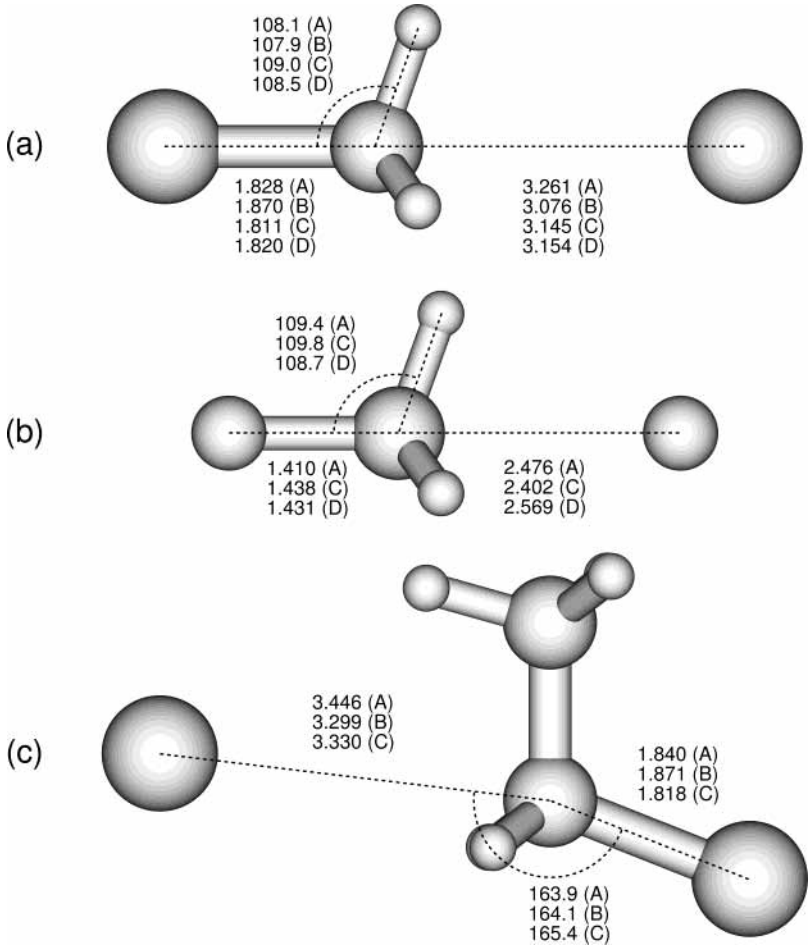

Figure 2. Key features of geometries for ion−dipole complexes in the gas-phase S_N2 identity reactions: (a) $CH_3Cl + Cl^-$; (b) $CH_3F + F^-$; (c) $CH_3CH_2Cl + Cl^-$. Calculations are labeled: (A) RHF/6-31G(d,p); (B) B3LYP/6-31G(d,p); (C) MP2/6-31G(d,p); (D) QCISD(T)/6-311++G(3df,-2p),[1] with bond lengths in angstroms and angles in degrees.

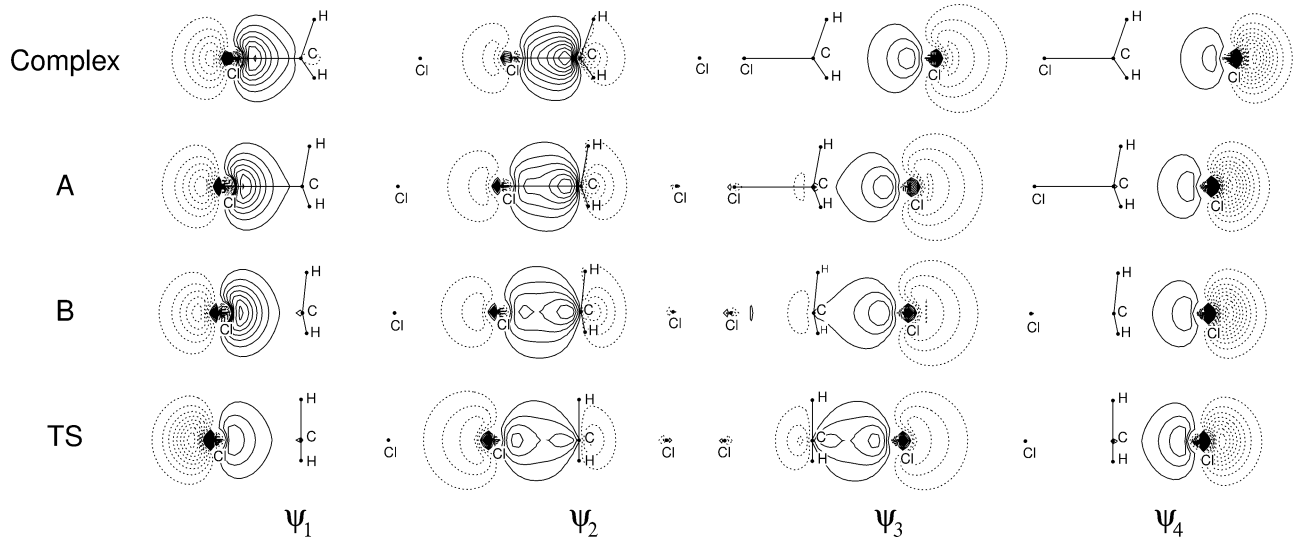

Figure 3. Active spin-coupled orbitals for the gas-phase S_N2 identity reaction of CH_3Cl and Cl^-. Successive rows correspond to the ion−dipole complex (top row), $R_{irc} = +1.19938$ amu$^{1/2}$ bohr (row A), $R_{irc} = +0.59953$ amu$^{1/2}$ bohr (row B), and the transition state, at $R_{irc} = 0$ amu$^{1/2}$ bohr (bottom row). Contour plots with a separation of 0.05 between the levels as produced by MOLDEN,[12] with dotted lines corresponding to negative values.

with total spin S and projection M) that is expanded in the full spin space, according to

$$\Theta_{SM}^{N} = \sum_{k=1}^{f_S^N} C_{Sk}\Theta_{SM;k}^{N} \qquad (2)$$

All of the variational parameters, namely the spin-coupling coefficients (C_{Sk}) in the Kotani basis[8,9] and the expansion coefficients of the active (ψ_μ) and inactive (ϕ_i) orbitals in the underlying 6-31G(d,p) basis set, were fully optimized simultaneously.[10] For a singlet system with four active orbitals, $f_0^4 = 2$, and the last (in this case, second) Kotani spin function, also

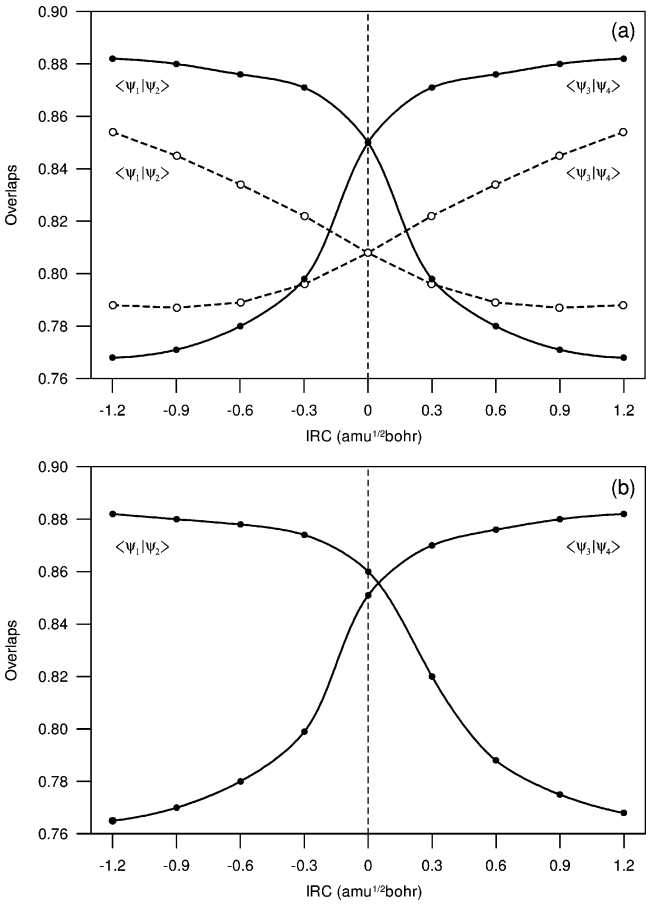

Figure 4. Variation with R_{irc} of the key active-space spin-coupled orbital overlap integrals $\langle\psi_1|\psi_2\rangle$ and $\langle\psi_3|\psi_4\rangle$ for gas-phase S_N2 identity reactions of RX and X^-. (a) $CH_3Cl + Cl^-$ (filled circles and full lines) and $CH_3F + F^-$ (open circles and broken lines); (b) $CH_3CH_2Cl + Cl^-$.

known as the "perfect-pairing" spin function,[8,9] is given by a particularly simple expression:

$$\Theta^4_{00;2} = {}^1/_2[\alpha(1)\,\beta(2) - \alpha(2)\,\beta(1)]\,[\alpha(3)\,\beta(4) - \alpha(4)\,\beta(3)] \quad (3)$$

SC(4) calculations were performed at the MP2(fc)/6-31G(d,p) geometry of the reactant-like ion−dipole complex, at the TS, and at several points along the corresponding IRC. As has been well documented,[7] such very compact SC(4) wave functions should only be very slightly inferior to the corresponding CASSCF(4,4) descriptions, but they are, of course, a great deal simpler to interpret directly in terms of familiar chemical concepts.

Results and Discussion

Geometries. Key features of the transition state geometries for the gas-phase S_N2 identity reactions $CH_3Cl + Cl^-$, $CH_3F + F^-$, $CH_3CH_2Cl + Cl^-$, and $C(CH_3)_3Cl + Cl^-$ are shown in Figure 1, and the corresponding geometries for reactant-like ion−dipole complexes are summarized in Figure 2. The structural parameters are taken from our RHF/6-31G(d,p), B3LYP/6-31G(d,p), and MP2(fc)/6-31G(d,p) calculations. Where available, results from the QCISD(T)/6-311++G(3df,2p) calculations of Lee et al.[1] are also shown. Our MP2 results for the various Cl^- systems are consistent with the MP2/6-31G(d) values reported by Jensen,[3] with relatively small differences being mostly due to the use here of a slightly more flexible basis set. The very large basis set CCSD(T) calculations of Gonzales et al.[2] for the $CH_3F + F^-$ reaction produced geometries that are similar to those of Lee and co-workers.[1]

The transitions states for the $CH_3Cl + Cl^-$ and $CH_3F + F^-$ reactions retain D_{3h} (trigonal bipyramidal) symmetry at all the different levels of theory. As mentioned earlier, and as shown in Figure 1c, the various correlated descriptions of the transition state for the $CH_3CH_2Cl + Cl^-$ system exhibit a small degree of asymmetry between the lengths of the making and breaking σ bonds. The same is not true of the RHF geometry, which features equal CCl distances and the methyl group rotated relative to the orientation shown in the figure. Analogous behavior is observed for the $C(CH_3)_3Cl + Cl^-$ system, with unequal CCl separations at correlated levels and with methyl groups rotated at the RHF level relative to the orientation shown in Figure 1d.

As can be seen from Figure 2a,c, the C−Cl bond lengths within the $Cl^-...CH_3CH_2Cl$ and $Cl^-...CH_3Cl$ ion−dipole complexes are very similar for geometries optimized at the same level of theory, but the C...Cl^- distances in $Cl^-...CH_3CH_2Cl$ are consistently longer, by about 0.2 Å, than those in $Cl^-...CH_3Cl$. In the case of $F^-...CH_3F$, the B3LYP/6-31G(d,p) geometry optimization failed to converge to a minimum but produced instead a second-order saddle point.

We turn now to the spin-coupled description of these various systems and to the changes that occur along the IRC, considering each reaction in turn.

SC Description of the S_N2 Identity Reaction of CH_3X and X^- (X = F or Cl). The shapes of the four active spin-coupled orbitals for the $CH_3Cl + Cl^-$ system are shown in Figure 3, with successive rows corresponding to the ion−dipole complex (top row), $R_{irc} \approx 1.2$ amu$^{1/2}$ bohr (row A) and $R_{irc} \approx 0.6$ amu$^{1/2}$ bohr (row B), and the transition state, at $R_{irc} = 0$ amu$^{1/2}$ bohr (bottom row). Because the IRC is symmetrical, there is of course no need to consider geometries on both sides of the TS. Starting with the ion−dipole complex (top row of Figure 3), we find that orbitals ψ_1 and ψ_2 are responsible for a very much fully formed C−Cl σ bond. These two orbitals have a high overlap (0.79), and the corresponding electron spins are almost exactly singlet coupled. Similarly, orbitals ψ_3 and ψ_4, which describe the lone pair on Cl^-, have a high overlap (0.885), and the spins are essentially coupled to a singlet. Moving toward the transition state, the initial changes to the orbitals are fairly modest, with relatively small changes to the two main overlap integrals, as illustrated in Figure 4a. All of the SC overlap integrals are listed in Table S1 (Supporting Information). The changes to the orbitals and to the overlap integrals become much more rapid as one approaches the TS, but the two "pairs" are essentially preserved, with predominantly perfect pairing of the electron spins. The overlap within each of the two equivalent "pairs" at the TS is 0.85.

We find a qualitatively similar SC description for $CH_3F + F^-$, as can be seen from the shapes of the orbitals in Figure 5, which is laid out in much the same way as was Figure 3 for the chlorine system. The overlaps within the predominantly singlet-coupled "pairs" are again illustrated in Figure 4a, with all of the overlap integrals listed in Table S2. A significant difference is that the bonding interactions between the incoming nucleophile and the carbon center develop at a somewhat earlier stage than in the chlorine case. Indeed, even at $R_{irc} \approx +1.2$ amu$^{1/2}$ bohr (second row of Figure 5), orbitals ψ_3 and ψ_4 are already clearly polarized in the direction of the C atom. There are also significant differences in the rates of forming the new carbon−halogen bond, as demonstrated by the changes to the orbitals and to the overlaps between them. We note also that the

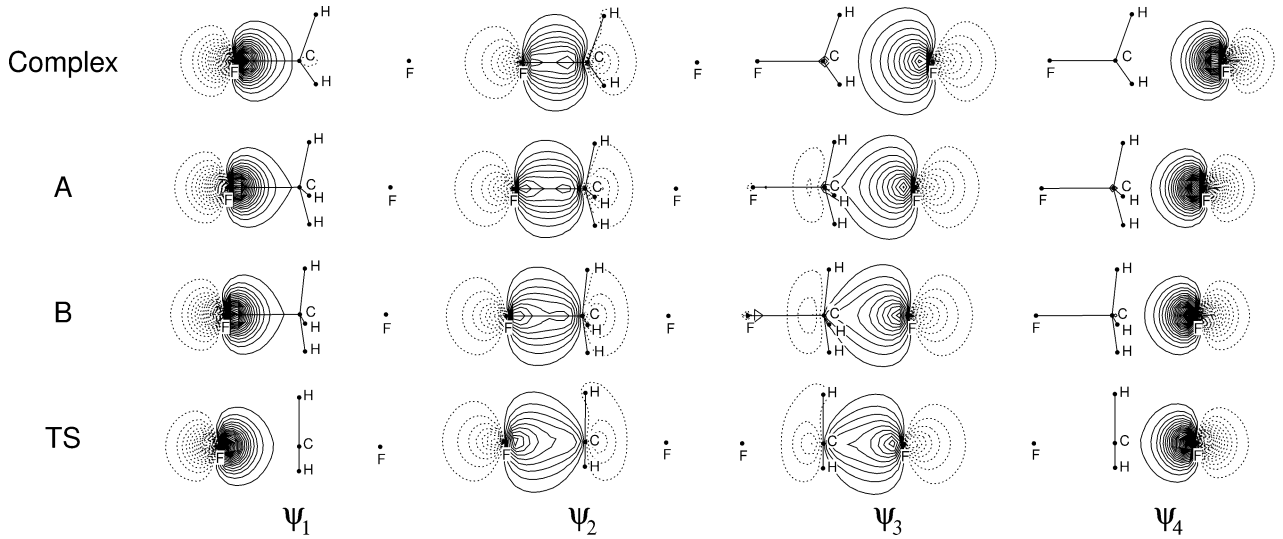

Figure 5. Active spin-coupled orbitals for the gas-phase S_N2 identity reaction of CH_3F and F^-. Successive rows correspond to the ion−dipole complex (top row), $R_{irc} = +1.19750$ amu$^{1/2}$ bohr (row A), $R_{irc} = +0.59765$ amu$^{1/2}$ bohr (row B), and the transition state, at $R_{irc} = 0$ amu$^{1/2}$ bohr (bottom row). Contour plots produced in the same fashion as in Figure 3.

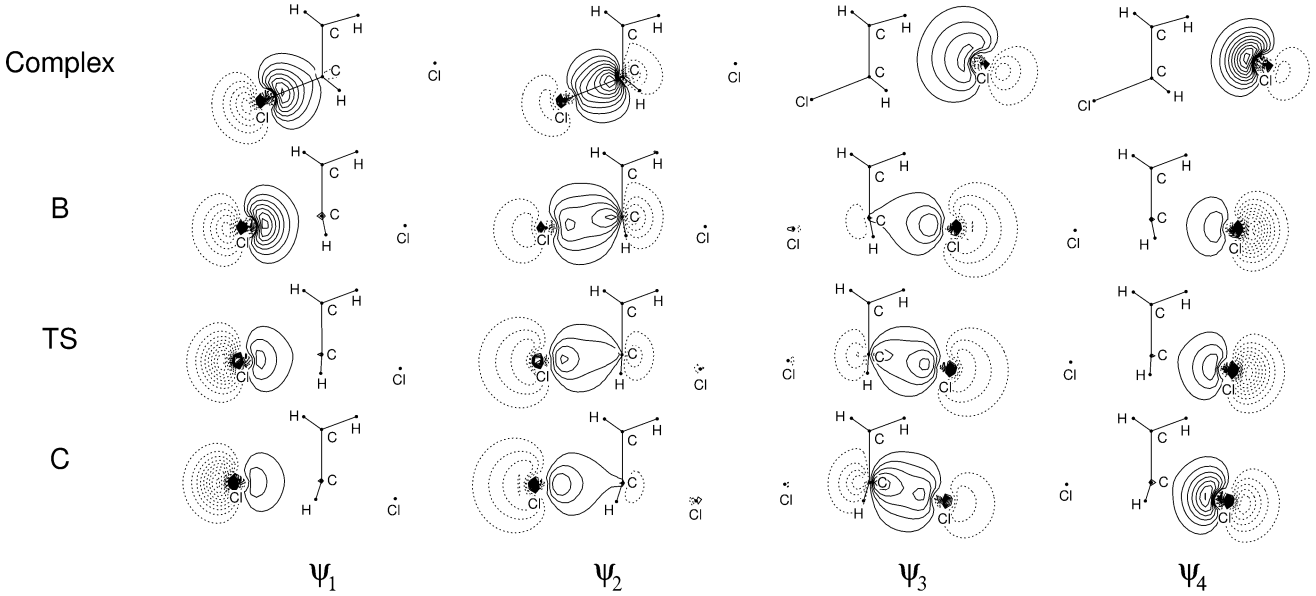

Figure 6. Active spin-coupled orbitals for the gas-phase S_N2 identity reaction of CH_3CH_2Cl and Cl^-. Successive rows correspond to an ion−dipole complex (top row), $R_{irc} = +0.59930$ amu$^{1/2}$ bohr (row B), the transition state ($R_{irc} = 0$ amu$^{1/2}$ bohr), and to $R_{irc} = 0.59933$ amu$^{1/2}$ bohr (bottom row). Contour plots produced in the same fashion as in Figures 3 and 5.

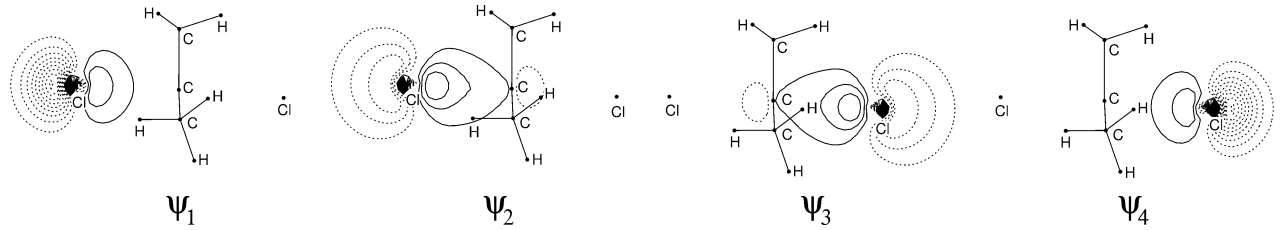

Figure 7. Active spin-coupled orbitals for the transition state of the gas-phase S_N2 identity reaction of $(CH_3)_3CCl$ and Cl^-. Contour plots produced in the same fashion as in previous figures.

magnitude of the (small) interpair overlap $\langle\psi_2|\psi_3\rangle$ is higher, reaching 0.25 at the TS, as compared to 0.11 for the chlorine system.

During the course of these $CH_3X + X^-$ reactions, $\langle\psi_1|\psi_2\rangle$ increases from a value *a*, characteristic of a C−X σ bond in the reactant-like complex, to a value *b*, characteristic of a lone pair in the product-like complex. Of course, $\langle\psi_3|\psi_4\rangle$ varies in the same way, but in the opposite direction. The two curves for the variation of these overlaps with R_{irc} (see Figure 4) cross at the transition state at an intermediate value, *c*. Lower values of the ratio $(c - a)/(b - a)$ indicate a higher degree of C−X bonding at the transition state, whereas higher values of the ratio correspond to a greater extent of a planar methyl cation sandwiched between two X^- anions. We find that this ratio is 0.1 for the fluorine reaction and 0.6 for the corresponding case of chlorine. This big difference shows us directly that there is a significantly larger extent of bond formation at the TS for the stronger nucleophile, F^-, as was also inferred for example by

Lee and co-workers,[1] by examining the changes in bond lengths from the reactants to the transition state.

SC Description of the S_N2 Identity Reaction of CH_3CH_2Cl and Cl^-. Changing the methyl group to an ethyl group leads to differences in the relative energies of the stationary points and to minor geometric changes, such as a transition state with a small degree of asymmetry between the lengths of the making and breaking bonds. Nonetheless, we find that the orbital descriptions of the two systems are very similar. The shapes of the four active spin-coupled orbitals for the $CH_3CH_2Cl + Cl^-$ system are shown in Figure 6, with successive rows corresponding to the reactant-like ion−dipole complex (top row), $R_{irc} \approx +0.6$ amu$^{1/2}$ bohr (row B), the transition state ($R_{irc} = 0$ amu$^{1/2}$ bohr), and to $R_{irc} \approx -0.6$ amu$^{1/2}$ bohr (bottom row). All of the corresponding overlap integrals are listed in Table S3.

Apart from the different orientation, there are significant similarities between the top rows of Figures 3 and 6 for these two Cl^-...R−Cl ion−dipole complexes (R = methyl or ethyl). We find that the overlaps $\langle\psi_1|\psi_2\rangle$, between the orbitals in the C−Cl bond, and $\langle\psi_3|\psi_4\rangle$, between the orbitals mostly responsible for the Cl^- lone pair, are largely unaffected by the presence of an additional methyl group. Such similarities persist along the reaction path, as is apparent both from the shapes of the orbitals and from the variation with R_{irc} of the two main overlap integrals, as is illustrated in Figure 4b. Indeed, the $\langle\psi_3|\psi_4\rangle$ curves for these two systems practically coincide. Approaching the TS from the reactant-like ion−dipole complex, the $\langle\psi_1|\psi_2\rangle$ curve for the ethyl system runs a little higher than that for the methyl reaction, corresponding to slightly faster breaking of the C−Cl σ bond, but the two curves become more similar on the product side.

We find for both of these $RCl + Cl^-$ systems that the active-space total spin function Θ^4_{00} is dominated over the whole IRC interval by the perfect-pairing mode of spin coupling. All in all, we may conclude that the switch from methyl to ethyl chloride has only a fairly minor influence on the qualitative form of the SC description for these gas-phase S_N2 identity reactions. The same turns out not to be true for the final system we considered, $C(CH_3)_3Cl + Cl$-.

SC Description of the S_N2 Identity Reaction of $C(CH_3)_3Cl$ and Cl^-. As a rule, *tert*-butyl chloride undergoes substitution reactions with nucleophiles in solution via an S_N1 mechanism, and so we restrict our attention on the gas-phase S_N2 reaction just to the transition state. It is clear from Figure 1 that the carbon−chlorine separations for this species are significantly longer than in the methyl and ethyl cases. The shapes of the four active spin-coupled orbitals for the transition state of the *tert*-butyl system, shown in Figure 7, give the impression of two Cl^- lone pairs. As in the other systems, we find two predominantly singlet-coupled pairs. The key overlaps, $\langle\psi_1|\psi_2\rangle$ and $\langle\psi_3|\psi_4\rangle$, both exceed 0.87; such a value is higher than we observed for the two smaller systems, and it can be compared with a typical value of 0.885 for the Cl^- lone pair in the ion−dipole complexes we have examined. The full set of overlap integrals is listed in Table S4.

Thus, the SC model for the TS of the S_N2 gas-phase identity reaction between $(CH_3)_3CCl$ and Cl^- can be described fairly accurately as involving a $(CH_3)_3C^+$ carbocation "clamped" between two Cl^- ions. This suggests a tendency for a switch from the S_N2 to the S_N1 mechanism. We cannot describe the latter within our gas-phase study, but it is obvious that in the presence of suitable solvent molecules the components of the TS would separate to form individual solvated $(CH_3)_3C^+$ and Cl^- ions. We note that Mohamed and Jensen[4] concluded that microsolvation causes only relatively small changes in the transition state geometries for the S_N2 identity reactions involving methyl, ethyl, and even isopropyl chloride but that the *tert*-butyl TS becomes significantly looser.

Discussions in organic chemistry textbooks, such as ref 11, of the influence of steric factors on reaction rates typically consider more S_N2 $RCl + Cl^-$ examples than we have examined in detail here. Probably the most common additional ones are the corresponding reactions of isopropyl and neopentyl chloride. As was mentioned earlier, our MP2(fc)/6-31G(d,p) transition state geometries for the gas-phase S_N2 identity reactions of methyl, ethyl, and *tert*-butyl chloride are in good agreement with the MP2/6-31G(d) results of Jensen.[3] As such, there are no reasons to expect that MP2-level calculations utilizing a slightly larger basis set, as in the current work, would introduce significant changes to any of the gas-phase MP2/6-31G(d) TS geometries[3] reported for the corresponding reactions of propyl, isopropyl, isobutyl, and neopentyl chloride. The full sequence of TS R−Cl separations calculated by Jensen[3] runs as follows: 2.307 Å (Me), 2.342/2.369 Å (Et), 2.356 Å (Pr), 2.355/2.391 Å (*i*-Bu), 2.405/2.412 Å (neo-Pen), 2.419 Å (*i*-Pr), and 2.604/2.637 Å (*t*-Bu). Whereas the variations in the gas-phase TS R−Cl distances for Me, Et, Pr, *i*-Bu, neo-Pen, and *i*-Pr are relatively small, the TS R−Cl separations for *t*-Bu are significantly larger. In light of this observation, it would be very surprising if the SC descriptions of the bond-breaking and bond-making processes in the gas-phase S_N2 identity reactions of propyl, isobutyl, neopentyl, and isopropyl chloride exhibited any notable differences from those we have presented here for the cases of methyl and ethyl chloride.

Summary and Conclusions

We have calculated RHF/6-31G(d,p), B3LYP/6-31G(d,p), and MP2(fc)/6-31G(d,p) geometries for the reactant-like ion−dipole complexes and for the transition states of the $CH_3Cl + Cl^-$, $CH_3F + F^-$, and $CH_3CH_2Cl + Cl^-$ gas-phase S_N2 identity reactions. Spin-coupled calculations along IRCs calculated at the MP2(fc)/6-31G(d,p) level reveal details of the electronic rearrangements taking place during the course of these reactions. We also examined the geometry and spin-coupled description of the gas-phase S_N2 transition state for the $(CH_3)_3CCl + Cl^-$ identity reaction and found significant differences from the other systems.

Although the SC descriptions of the $CH_3Cl + Cl^-$ and $CH_3F + F^-$ gas-phase S_N2 identity reactions are qualitatively similar, we find a significantly larger extent of bond formation at the TS for the fluorine case; the electronic rearrangements also start much sooner. Comparing the $CH_3Cl + Cl^-$ and $CH_3CH_2Cl + Cl^-$ systems, our spin-coupled calculations along the IRCs suggest that the electronic structure reorganization is largely unaffected by the presence of the additional methyl substituent at the carbon site. However, the SC description of the TS for the reaction involving *tert*-butyl chloride as substrate is radically different: it is most consistent with the idea of a carbocation "clamped" between two chloride ions, with only relatively weak covalent interactions.

Supporting Information Available: Tables of overlap integrals between active SC orbitals. This material is available free of charge via the Internet at http://pubs.acs.org.

References and Notes

(1) Lee, I.; Kim, C. K.; Sohn, C. K.; Li, H. G.; Lee, H. W. *J. Phys. Chem. A* **2002**, *106*, 1081.

(2) Gonzales, J. M.; Pak, C.; Cox, R. S.; Allen, W. D.; Shaefer, H. F.; Császár, A. G.; Tarczay, G. *Chem.—Eur. J.* **2003**, *9*, 2173.

(3) Jensen, F. *Chem. Phys. Lett.* **1992**, *196*, 368.

(4) Mohamed, A. A.; Jensen, F. *J. Phys. Chem. A* **2001**, *105*, 3259.

(5) Gonzalez, C.; Schlegel, H. B. *J. Chem. Phys.* **1989**, *90*, 2154. (b) Gonzalez, C.; Schlegel, H. B. *J. Phys. Chem.* **1990**, *94*, 5523.

(6) Frisch, M. J.; Trucks, G. W.; Schlegel, H. B.; Scuseria, G. E.; Robb, M. A.; Cheeseman, J. R.; Zakrzewski, V. G.; Montgomery, J. A.; Stratmann, R. E.; Burant, J. C.; Dapprich, S.; Millam, J. M.; Daniels, A. D.; Kudin, K. N.; Strain, M. C.; Farkas, O.; Tomasi, J.; Barone, V.; Cossi, M.; Cammi, R.; Mennucci, B.; Pomelli, C.; Adamo, C.; Clifford, S.; Ochterski, J.; Petersson, G. A.; Ayala, P. Y.; Cui, Q.; Morokuma, K.; Malick, D. K.; Rabuck, A. D.; Raghavachari, K.; Foresman, J. B.; Cioslowski, J.; Ortiz, J. V.; Baboul, A. G.; Stefanov, B. B.; Liu, G.; Liashenko, A.; Piskorz, P.; Komaromi, I.; Gomperts, R.; Martin, R. L.; Fox, D. J.; Keith, T.; Al-Laham, M. A.; Peng, C. Y.; Nanayakkara, A.; Gonzalez, C.; Challacombe, M.; Gill, P. M. W.; Johnson, B.; Chen, W.; Wong, M. W.; Andres, J. L.; Head-Gordon, M.; Replogle, E. S.; Pople, J. A. *Gaussian 98, Revision A.7*; Gaussian, Inc.: Pittsburgh, PA, 1998.

(7) Cooper, D. L.; Gerratt, J.; Raimondi, M. *Chem. Rev.* **1991**, *91*, 929. (b) Gerratt, J.; Cooper, D. L.; Karadakov, P. B.; Raimondi, M. In *Handbook of Molecular Physics and Quantum Chemistry*; Wilson, S., Ed.; Wiley: Chichester, 2003; Vol. 2, Part 2, Chapter 12, pp 148−68.

(8) Kotani, M.; Amemyia, A.; Ishiguro, E.; Kimura, T. *Tables of Molecular Integrals*; Maruzen: Tokyo, 1963.

(9) Pauncz, R. *Spin Eigenfunctions*; Plenum: New York, 1979.

(10) Karadakov, P. B.; Gerratt, J.; Cooper, D. L.; Raimondi, M. *J. Chem. Phys.* **1992**, *97*, 7637.

(11) Solomons, T. W. G.; Fryhle, C. B. *Organic Chemistry*, 7th ed.; Wiley: New York, 2000.

(12) Schaftenaar, G. *MOLDEN (A Pre- and Post Processing Program of Molecular and Electronic Structure)*, CAOS/CAMM Center, The Netherlands.